buildings

MDPI

Article

High-Cycle Fatigue Properties of Titanium-Clad Bimetallic Steel with Different Interfacial Conditions

Jianbo Jiang [1,2], Chenyang Huang [3], Huiyong Ban [3,*] and Letian Hai [3]

[1] State Key Laboratory of Metal Material for Marine Equipment and Application, Anshan 114009, China
[2] Ansteel Beijing Research Institute Co., Ltd., Beijing 102209, China
[3] Department of Civil Engineering, Tsinghua University, Beijing 100084, China
* Correspondence: banhy@tsinghua.edu.cn; Tel.: +86-10-62773505

Abstract: Titanium-clad (TC) bimetallic steel is an advanced composite steel consisting of metallurgically bonded titanium alloy and structural steel. This paper compared the high-cycle fatigue properties of three types of TC bimetallic steels, including two hot-rolled bonding types with different bonding strengths and an explosion-bonded type. The three types of TC bimetallic steels were all manufactured from TA2 titanium alloy as the cladding metal and Q355B structural steel as the substrate metal, of which the thicknesses are 2 mm and 8 mm, respectively. Based on the comparison results, the qualitative relationship between the bonding interface strength and the manufacturing methods with the basic mechanical and high-cycle fatigue properties was obtained. It was found that the different manufacturing methods and the bonding degree of the two component metals resulted in the different nonlinear yield plateau in the TC bimetallic steel. The high bonding strength seems to affect the failure mode of the tensile coupons. The bonding interface shear strength only slightly affects the tensile performance, which exhibits visible effects only when the test strain reaches the fractured state. In addition, three failure modes in total were found in the high-cycle fatigue tests for the three types of TC bimetallic steel. The manufacturing methods and the bonding interface strength significantly affect the fatigue phenomena of the TC bimetallic steel. The hot-rolled bonding TC bimetallic steel with high bonding strength has a 10% improvement in fatigue performance than the one with low bonding strength. Despite this, the manufacturing methods significantly affect the fatigue ratio, while the influence of the bonding strength on the high cycle fatigue performance is limited. The research outcomes can provide reference for the selection of different manufacturing methods and interfacial conditions for the use of TC bimetallic steel in structural engineering.

Keywords: titanium-clad bimetallic steel; fatigue; basic mechanical properties; interfacial conditions

check for updates

Citation: Jiang, J.; Huang, C.; Ban, H.; Hai, L. High-Cycle Fatigue Properties of Titanium-Clad Bimetallic Steel with Different Interfacial Conditions. *Buildings* **2023**, *13*, 758. https://doi.org/10.3390/buildings13030758

Academic Editor: Harry Far

Received: 27 February 2023
Revised: 9 March 2023
Accepted: 13 March 2023
Published: 14 March 2023

Copyright: © 2023 by the authors. Licensee MDPI, Basel, Switzerland. This article is an open access article distributed under the terms and conditions of the Creative Commons Attribution (CC BY) license (https://creativecommons.org/licenses/by/4.0/).

1. Introduction

Titanium-clad (TC) bimetallic steel [1], an advanced composite steel consisting of metallurgically bonded titanium alloy and structural steel, has been widely used for tube sheets mainly because of the high corrosion resistance of titanium alloy and favorable mechanical properties of the structural steel [2]. Usually, structural steel is used as a substrate metal, and titanium alloy is used as a cladding metal, as shown in Figure 1. With the comparable production cost and higher corrosion resistance to austenitic stainless steel, the TC bimetallic steel has been widely used in the petroleum and chemical industries, and seawater desalination [2]. Given its excellent properties, TC bimetallic steel can also yield huge application potential in civil and structural engineering in the marine environment due to its outstanding structural performance, environmental friendliness, and full-life-cycle economy advantages. The primary manufacturing method of this bimetallic steel is the explosion bonding and hot-rolled bonding processes [3]. The explosion bonding is a solid-state metal joining process with detonation accelerating the cladding metal plate to a velocity at which a metallurgic bond is formed between the metals during collision [4]. While the hot-rolled bonding process is a more adequate and stable manufacturing

method [5], through which a metallurgic bond is formed by the achievement of diffusion between the substrate and cladding metals [3]. At present, both manufacturing methods for TC bimetallic steel have been thoroughly studied [3–8], and the basic mechanical properties of TC bimetallic steel have also been preliminarily studied [9–11]. Studies investigating hot-rolled bonding TC bimetallic steel fatigue behavior are relatively limited [12,13]. Meanwhile, some investigations have studied the fatigue behavior of explosion-bonded TC bimetallic steel [14–17]. The fatigue design curve for explosion-bonded TC bimetallic has been proposed, with the fatigue propagation mechanism has been analyzed [16]. It has been indicated that the high-cycle fatigue properties of explosion-bonded TC bimetallic steels are in between compared with that of the two component metals [17]. Despite this, the existing fatigue studies are still insufficient to deeply understand the high-cycle fatigue mechanism of the TC bimetallic steel, or to clarify the influence of manufacturing methods and interfacial conditions on the mechanical properties of the TC bimetallic steel.

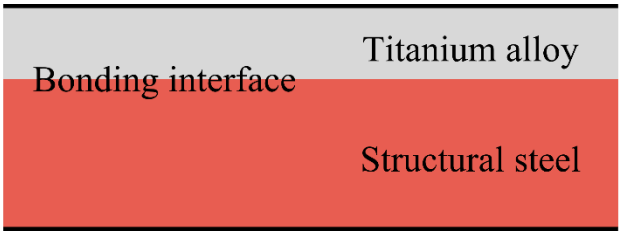


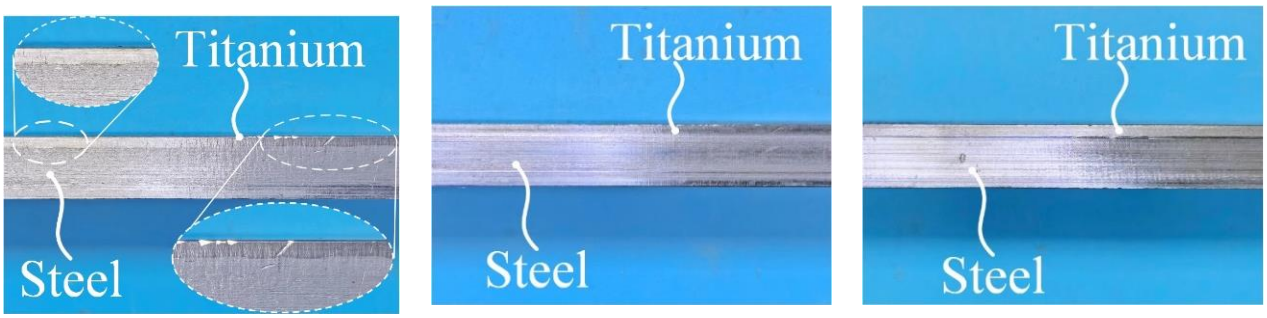
Figure 1. Illustration of TC bimetallic steel.

Therefore, this paper mainly aims to compare high-cycle fatigue test results [12,16] that were carried out on three types of specimens made of TC bimetallic steel with two different manufacturing methods, namely explosion bonding, and hot-rolled bonding processes. Among them, two types of specimens are produced by the hot-rolled bonding process, but with various grades of bonding strength. The basic mechanical properties, including tensile performance and shear strengths at the bonding interface, are also compared in this paper. Based on the comparison results, the influence of different interfacial properties on the fatigue behavior of TC bimetallic steel is elucidated, and several fatigue fracture modes of the bimetallic steel are summarized. The research outcomes can provide reference for selecting different manufacturing methods and interfacial conditions in the use of TC bimetallic steel in structural engineering.

2. Review of Previous Experimental Investigations

The investigated specimens were sampled from two hot-rolled bonding TC bimetallic steel plates (with 40 MPa and 200 MPa interface shear strength grades, respectively) and an explosion-bonded TC bimetallic steel plate. A total of three plates were all manufactured by bonding TA2 titanium alloy (GB/T 3621-2007 [18]) and Q355B steel plates (GB/T 50017-2017 [19]), which are 2mm and 8mm thick, respectively. It is worth noting that the cladding metal and substrate metal in the three types of TC bimetallic steel with the same grade are not from the same batch. Given the fact that these three materials with different interface conditions were not prepared at one time, the size of the specimens in different groups was adjusted during the preparation. All the specimens' size conforms to the corresponding design standards, and the difference does not affect the comparison of the experimental results. The test data that were used in this paper were all extracted from the previous studies under similar test conditions, which has been reported in detail previously [12,16]. Figure 2 shows the interfacial conditions in different types of the TC bimetallic steels. The interface of the explosion-bonded specimen presents an irregular wave texture with the cladding and the substrate metals blending with each other, which probably results in more potential defects in the bonding interface, as shown in Figure 2a. While the interface of the hot-rolled bonding specimen, whether the bonding grade is low or high, is relatively flat, and almost no macroscopic defects can be observed at the bonding

interface, as shown in Figure 2b,c. The characteristics of the bonding interface depend on the manufacturing methods. Explosion bonding is carried out through a progressive impulse resulting from a short duration release of high energy from an explosion [3,4]. Plastic deformation is caused by non-uniform pressure at the bonding interface, resulting in the cladding metal and the base metal blending. In the hot-rolled bonding process, the metallic bond is formed by the achievement of diffusion between the substrate and cladding metals [3], which has more a stable quality due to the adequacy of the hot-rolling process [20], resulting in a flat bonding interface. To distinguish the three types of materials that were investigated herein, the designation of test specimens includes the manufacturing methods and interface bonding conditions. For example, specimen HCF-HR-LBS-1 represents a high-cycle fatigue (HCF) test specimen that was manufactured by the hot-rolling (HR) process with low bonding strength (LBS). The last number in the designation denotes the serial number in the group.



(**a**) (**b**) (**c**)

Figure 2. Interfacial conditions in different types of the TC bimetallic steels: (**a**) explosion-bonded specimen; (**b**) hot-rolled bonding specimen with low bonding strength; and (**c**) hot-rolled bonding specimen with high bonding strength.

2.1. Basic Mechanical Properties Tests

Uniaxial tensile coupon tests and bonding interface shear tests were conducted previously [12,16] to obtain the experimental stress-stain curves and the interfacial shear strength of the three types of TC bimetallic steels. The tensile coupon tests were conducted in accordance with GB/T 228.1-2010 [21], which is generally equivalent to the international standards ISO 6892-1:2019 [22]. Figure 3 shows the nominal geometric dimensions of tensile coupon specimens, of which two kinds of standard specimens were designed for different types of materials. The influence of different coupons' size can be ignored due to standard specimens. There were three repeated specimens (labelled as TC-EB-HBS-1~3, TC-HR-HBS-1~3, and TC-HR-LBS-1~3) that were loaded for each type of specimen. The testing machine's chuck clamped the specimen at both ends of the straight section to employ force on it. The test stopped when the specimen ultimately fractured, and the testing machine recorded the force value during the test. The strain control of $0.025\%s^{-1}$ was employed during all these three testing procedures, which eliminates the effects of loading rate on the test result comparisons. The tensile coupon tests were conducted by using the Instron59 testing machine (for TC-EB-LBS and TC-HR-LBS) and the WE-100B testing machine (for TC-HR-HBS). The input parameter of both testing machines is the deformation rate, which can be calculated by to multiplying the strain rate and the parallel length of the specimens. For each tensile coupon test, two strain gauges and a clip-on extensometer were used to measure the longitudinal strain of the specimen in the early and late loading stages, respectively. It is worth noting that the strain measuring instrument was removed before the eventual fracture of the TC-HR-HBS specimens, resulting in the necking stage not being included in the stress-strain curves in this test. However, the obtained curves are sufficient for analyzing the stress-strain curve-related parameters and the mechanical properties of this material.

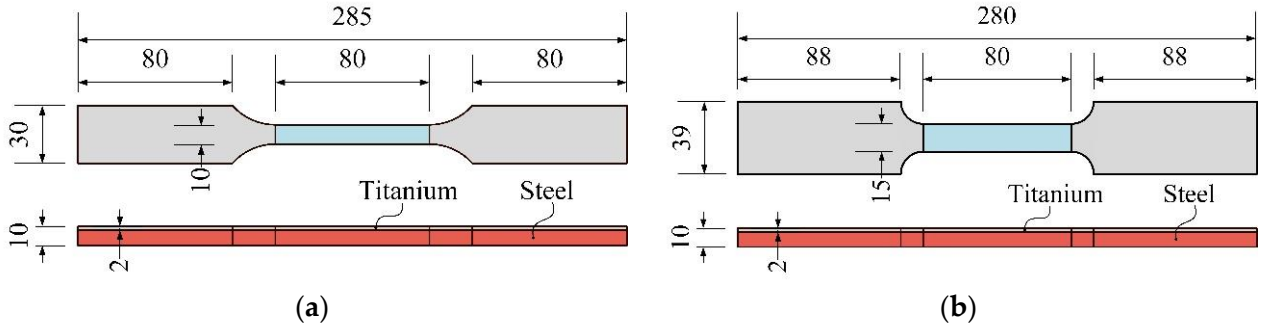


Figure 3. Tensile coupon test specimens: (**a**) TC-EB-HBS and TC-HR-LBS; (**b**) TC-HR-HBS.

The shear strength is one of the most important parameters for evaluating the quality of the bonding interface [23]. It was tested through bonding interface shear tests in accordance with the Chinese standard GB/T 6396-2008 [23]. The standard shear test specimens were used, as illustrated in Figure 4, and loaded with a rate of 0.5 N/s. An auxiliary device was used to carry out the shear tests [16], with the cladding metal placed on a platform and the base metal suspended. The testing machine pressed the base metal to make the cladding metal fall off the specimen. The peak load that was generated in the test process was considered as the specimen's interfacial shear capacity. The bonding interface shear strength was obtained through dividing the peak load by the shear interface's area of the specimen. A total of three or four repeated specimens (ST-HR-HBS-1~4, ST-HR-LBS-1~4, and ST-EB-HBS-1~3) were tested for each type of material.

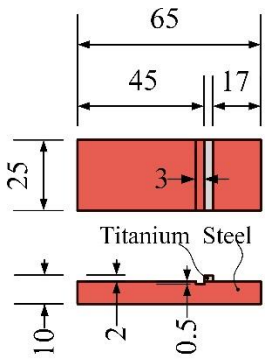


Figure 4. Shear test specimens.

2.2. High-Cycle Fatigue Tests

Uniaxial high cycle fatigue tests were undertaken on the three types of TC bimetallic steel previously (some have been published [12,16] and some are under review) according to GB/T 3075-2008 [24]. The geometric dimensions of the fatigue test specimens are shown in Figure 5, which are only different in the clamping end's length. The surfaces of all the specimens were polished to the same roughness conditions (*Ra* less than 0.2 μm). All the tests were conducted by using the QBG-250 fatigue test machine under a force-controlled system. The fatigue test is conducted by inputting the design mean stress and stress amplitude into the testing machine. The static load is applied on the specimen first to make the stress in the specimen reach the design mean stress, and then the dynamic load is applied to make the corresponding cyclic stress in the specimen. After the failure of the specimen, the fatigue test is terminated automatically with the self-protection system of the testing machine. The stress ratio for all the specimens was set to be 0.1, which may avoid other types of damage such as buckling, as well as the influence of average stress. A total of 20 specimens (HCF-HR-HBS-1~20, HCF-HR-LBS-1~20, and HCF-EB-HBS-1~20) were tested for each type of the material, for which five different stress levels were selected by the trial tests. The test was repeated four times at each stress level to ensure replication.

To avoid the case of infinite fatigue life of the specimen leading to long time loading, the cut-off limit was set to be 5 million cycles for the fatigue life of the specimens in accordance with GB 50017-2017 [19].

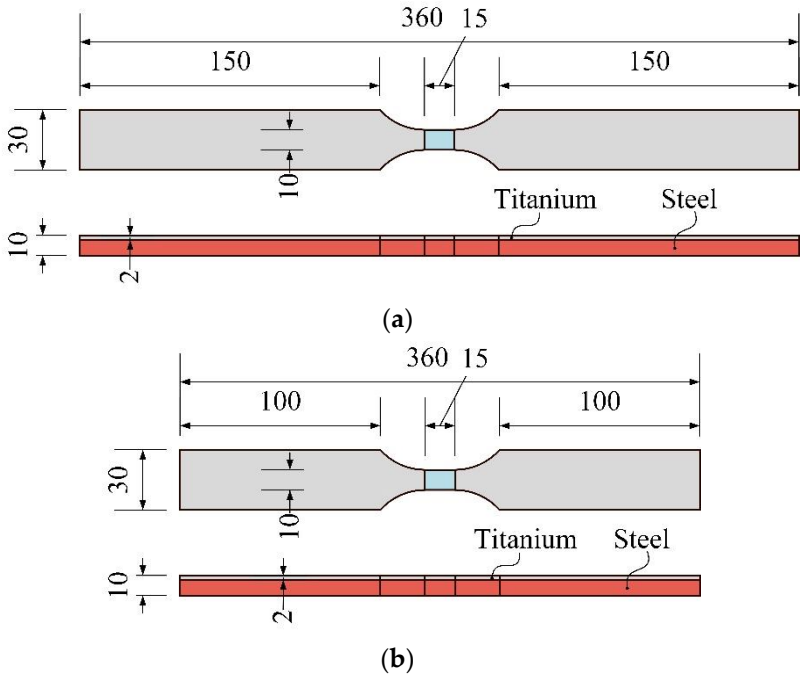


Figure 5. Geometry of high-cycle fatigue test specimens: (**a**) HCF-EB-HBS and HCF-HR-LBS; (**b**) HCF-HR-HBS [16].

3. Comparison and Discussions

3.1. Comparison of Basic Mechanical Properties

Figure 6 shows stress-strain curves of different TC bimetallic steels that were reported in the authors' previous studies [12,16], and comparisons of the typical stress-strain curves for different types of materials are depicted in Figure 7. Apparently, for explosion-bonded specimens such as TC-EB-HBS-1, a visible yield plateau followed by a strain hardening curve can be observed in the full-range stress-strain curve. For the hot-rolled bonding specimens with low bonding strength, such as Specimen TC-HR-LBS-1, the yield region exhibits strain-hardening behavior rather than a perfect flatness that is commonly found in the stress-strain curve of conventional structural steel; while for the hot-rolled bonding specimens with higher bonding grade such as TC-HR-HBS-1, the slope of its yield region is found to be intermediate between the afore-mentioned two curves (TC-EB-HBS-1 and TC-HR-LBS-1). The titanium alloy in the TC bimetallic steel possesses a representative nonlinearity in its full-range stress-strain curve [9]. It seems that the different manufacturing methods and bonding degrees of the two component metals result in the different nonlinear yield response in the TC bimetallic steel. It is worth noting that the three types of TC bimetallic steels employed substrate and cladding metals from different batches, which may also produce different effects on the three materials. For explosion-bonded specimens, the basic mechanical properties vary with the sampling locations, such as TC-EB-HBS-3.

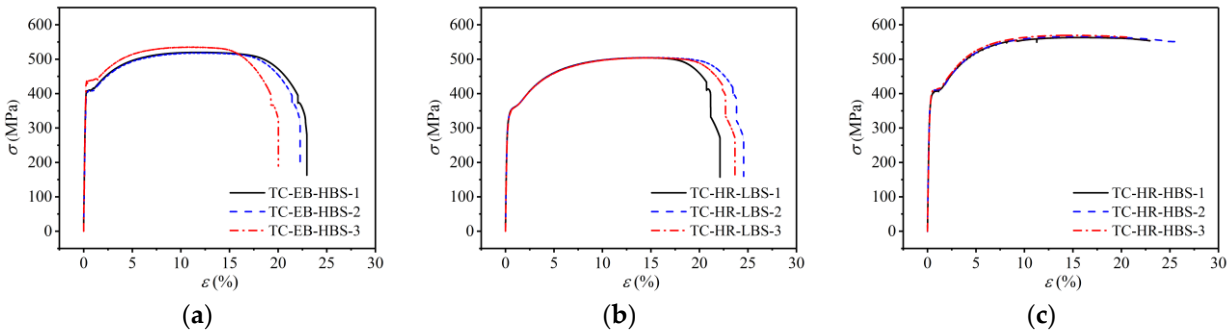


Figure 6. Stress-strain curves of specimens: (**a**) TC-EB-HBS-1, 2 and 3; (**b**) TC-HR-LBS-1, 2 and 3; and (**c**) TC-HR-HBS-1, 2 and 3.

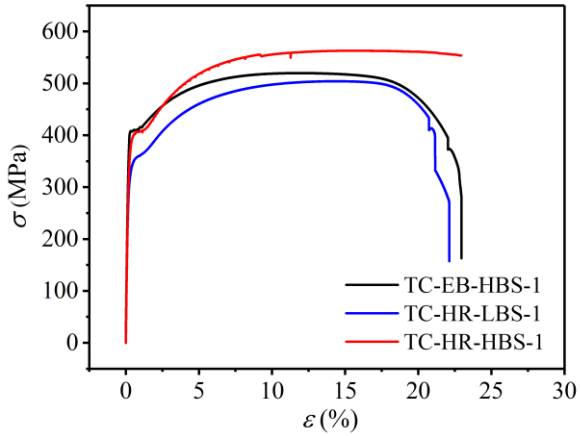


Figure 7. Comparison of typical experimental stress-strain curves for different kinds of the specimens.

In addition, it can be observed in Figure 6a that two sudden drops exist at the very late stage in the stress-strain curves of TC-EB-HBS, which corresponds to the separation at the bonding interface and the eventual fracture of the specimen, respectively. While Figure 6b shows three sudden drops at the same strain stage in the stress-strain curves of TC-HR-LBS, which correspond to the interface separation, titanium alloy fracture, and structural steel fracture. Although the stress-strain curves of TC-HR-HBS in Figure 6c do not show the fracture curve at the very late stage (which was not recorded due to removal of extensimeter), it can be seen from the existing curves that the strength of the explosion-bonded specimen decreases rapidly in the necking stage, while the hot-rolled bonding specimen has better ductility. Moreover, the bonding interfaces of all the three types of materials separated prior to the fracture, and the cladding and substrate metals generally failed simultaneously just right after the separation, which has a slight influence on the full-range behavior of the stress-strain responses. The reason for the two component metals of TC-HR-LBS to fracture successively is likely to be caused by low interface strength, which will be analyzed in detail with the following comparison of the interface shear strengths.

Table 1 shows the shear strengths at the bonding interface for three types of TC bimetallic steels, of which the average value of ST-HR-LBS is lower than the limit value (i.e., 140 MPa) in accordance with GB/T 8547-2019 [1]. Due to the uncertainties in terms of bonding qualities by the explosion bonding process, the measured value of ST-EB-HBS-3 is lower than the limit value, despite the average of the explosion-bonded specimens meeting the requirement. It seems that with higher bonding interface strength, the deviation of the shear strengths become higher. Theoretically, the shear test specimen has an interface with a specific thickness, of which part of the cladding layer needs to be milled to the interface position, as shown in Figure 4. However, the thickness of the bonding interface is too small to be perfectly recognized, as shown in Figure 2, which makes it difficult to ensure the

milled surface falls precisely at the bonding interface during processing. When the bonding strength is large enough, it becomes more difficult to ensure that the shear failure occurs at the bonding interface during the shear tests, which causes a significant standard deviation. Therefore, future studies need to add more repeated specimens in the bonding interface shear test. Both the mean and minimum values in the test results need to be focused on judging whether the interface quality meets the standard.

Table 1. Shear strengths at the bonding interface.

Specimens Serial Number	Shear Strengths (MPa)		
	ST-EB-HBS	**ST-HR-LBS**	**ST-HR-HBS**
1	160.6	58.1	271.1
2	148.0	35.4	148.8
3	133.5	37.6	237.8
4	-	34.1	215.3
Average value	147.3	41.3	218.3
Standard deviation	11.1	9.8	44.7
Limit value		140.0	

Table 2 shows the stress-strain curve-related parameters of the three types of TC bimetallic steel. All the average mechanical properties herein meet the requirements in accordance with GB/T 8547-2019 [1]. Comparison of these properties with variation of shear strengths demonstrates that the bonding interface strength has only a slight effect on the tensile mechanical properties, because the effect becomes visible only when the test strain reaches a fracture state, as shown in Figure 6.

Table 2. Average values of the measured mechanical properties.

Specimens	$\sigma_{0.2}$ (MPa)	σ_u (MPa)	E (GPa)	A (%)
TC-EB-HBS	414.8	524.4	193.4	33.7
TC-HR-LBS	338.4	504.3	172.9	30.9
TC-HR-HBS	395.1	566.1	185.0	31.4

3.2. Comparison of High-Cycle Fatigue Failure Phenomena

Figure 8 shows typical fracture photos of the three types of fatigue specimens, which can be classified into three failure modes. In the first one, the fatigue crack initiation occurs at the interface. Since the cladding metal is much thinner than the substrate one, crack propagation preferentially penetrates the cladding metal despite the titanium alloy possessing better fatigue resistance, as shown in Figure 8a,b,e. In the second one, the fatigue crack initiation occurs at the surface of the substrate steel due to the better fatigue resistance of the cladding titanium alloy, as shown in Figure 8c,d. The third one is the combination of the above two, and a penetrating crack is formed in the middle of the substrate metal, as shown in Figure 8f. Table 3 shows the number of specimens corresponding to each failure mode, including the number of undamaged specimens. The explosion-bonded TC bimetallic steel mainly failed in the way of the first failure mode, with a fracture of the entire cladding metal and a majority of the substrate metal, as shown in Figure 8a. The explosion bonding-process may result in more potential imperfections at the bonding interface [25], which is why explosion-bonded TC bimetallic steel failed in the way of the first failure mode. There were two failure modes that were found in the specimens of hot-rolled bonding TC bimetallic steel with low interfacial shear strength, as shown in Figure 8b,c. The hot-rolling process maintains the high quality of the bonding interface, resulting in more crack initiation occurring at the surface of the substrate steel. However, low interfacial shear strength still makes the interface a potential imperfection for crack propagation, resulting in more than a quarter of the specimens failing in the way of the

first failure mode. For hot-rolled bonding TC bimetallic steel with high bonding strength, despite the first two failure modes, as shown in Figure 8d,e, one more failure mode with two fatigue crack initiations was found in this kind of specimen, as shown in Figure 8f. The following section will illustrate the fatigue *S-N* curves of these three types of materials, of which the hot-rolled bonding specimens with high bonding strength are subjected to larger stress levels during the high-cycle fatigue tests due to its better fatigue property than the other two materials'. Therefore, two crack initiations are more likely to propagate simultaneously. The apparent separation was observed at the bonding interface only in the hot-rolled specimens with low bonding strength. Due to the test equipment self-protection system, the specimens were not entirely fractured after the fatigue test. In conclusion, the manufacturing methods and the bonding interface strength greatly affect the high-cycle fatigue phenomena of TC bimetallic steel. In addition, previous research [13] has shown that if the specimens maintained the original roughness (i.e., hot-rolled surfaces), the second failure mode with fatigue cracks initiating at the surface of the substrate steel would occur in most cases. This proves that the bonding interface and the surface roughness are two significant factors affecting the high-cycle fatigue properties of the TC bimetallic steel.

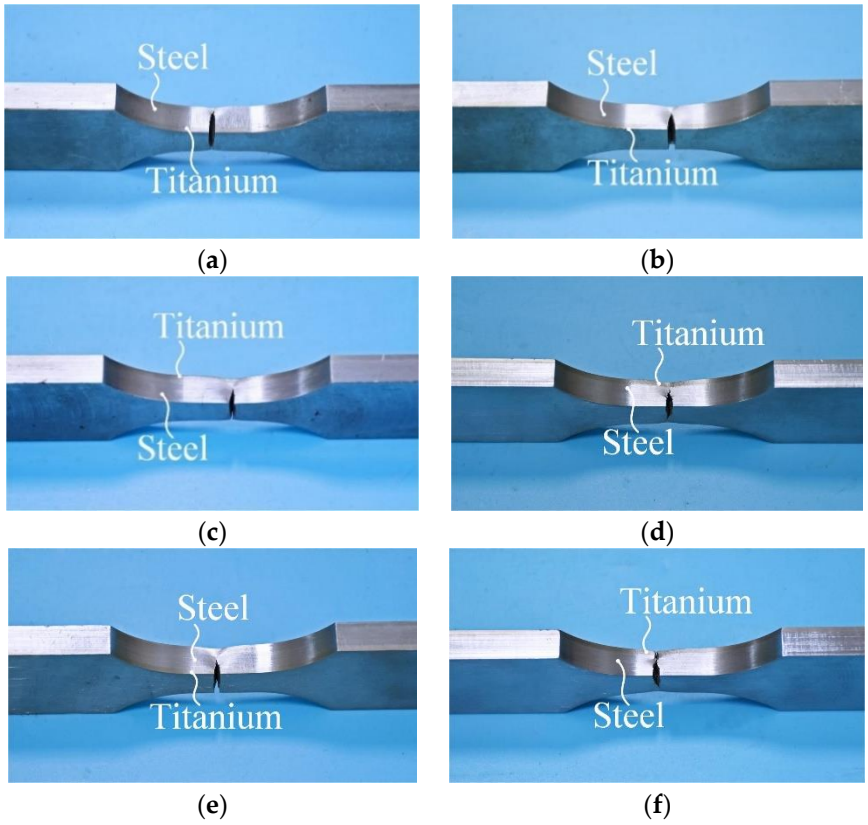


Figure 8. Failure modes that were observed in fatigue tests: (**a**) HCF-EB-HBS-7 (nominal maximum stress: 400 MPa); (**b**) HCF-HR-LBS-5 (nominal maximum stress: 370 MPa); (**c**) HCF-HR-LBS-12 (nominal maximum stress: 390 MPa); (**d**) HCF-HR-HBS-5 (nominal maximum stress: 430 MPa); (**e**) HCF-HR-HBS-14 (nominal maximum stress: 422.5 MPa); and (**f**) HCF-HR-HBS-8 (nominal maximum stress: 430 MPa).

Table 3. The number of the failure specimens.

Failure Mode	Number of the Specimens		
	HCF-EB-HBS	**HCF-HR-LBS**	**HCF-HR-HBS**
The first one	18	6	10
The second one	-	13	7
The third one	-	-	3
Undamaged one	2	1	-

As shown in Table 4, the test results show that the first and the second failure modes were not significantly affected by the stress level, while the third failure mode tends to occur under high fatigue stress levels. This indicates that minor defects are more likely to develop into cracks when the stress level is large, while this process is generally limited when the stress level is small. The single crack source generally occurs at a low stress level, while the two defects expand simultaneously at a high stress level. Nevertheless, more test data are needed for further analysis on the relationship between the failure modes and the stress level.

Table 4. The number of specimens HCF-HR-HBS for each failure mode.

Stress Level (MPa)	Number of the Specimens		
	The First Failure Mode	**The Second Failure Mode**	**The Third Failure Mode**
430	1	1	2
422.5	4		
415	1	2	1
410	2	2	
407.5	2	2	

3.3. Comparison of High-Cycle Fatigue Properties

Figure 9 shows the comparison of the fatigue *S-N* curves for the three types of TC bimetallic steel. Previous studies [12,16] have proven that the curves that were obtained from the high cycle fatigue tests are higher than the fatigue design curves of structural steel given in GB 50017 [19], Eurocode 3 [26], ANSI/AISC 360 [27] and BS 7608 [28], which demonstrates the existing design *S-N* curves are conservative for the TC bimetallic steel with all the three interfacial conditions. As shown in Figure 9, the distribution of the data and the fitting curves show that the fatigue strength of HCF-HR-HBS is higher than that of HCF-EB-HBS and is much higher than that of HCF-HR-LBS generally. However, this is not the case for a small part of the data, due to the discreteness of fatigue performance.

According to the Pearson correlation coefficients that are summarized in Table 5 and the failure mode numbers in Table 3, it seems that the fewer the failure modes are, the better the linear correlation between the material's fatigue life and strength is. The previous section has analyzed the characteristics of different fatigue failure modes. It is still worth noting that the mechanism of different failure modes is quite different in terms of the location of the fatigue crack initiation and the path of crack growth, leading to different ways for energy to form unstable cracks. Even specimens with completely identical internal defects would have different fatigue lives when different failure modes occurring in these specimens, so more failure modes would reduce the linear correlation of the fitting curve.

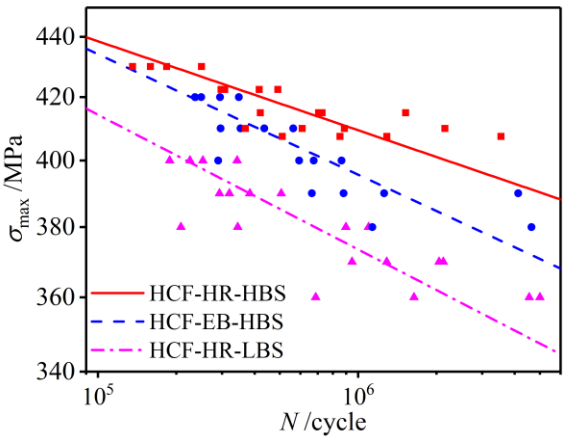


Figure 9. Comparison of the fatigue *S-N* curves for TC bimetallic steel with various interfacial conditions.

Table 5. Comparison of the fatigue behavior.

Specimens	*S-N* Curve Expression	*r*	$\sigma_{2\times10^6}$ (MPa)	σ_u (MPa)	Shear Strength (MPa)
HCF-HR-HBS	$\lg N + 33.6\lg\sigma_{max} = 93.8$	−0.794	401.9	566.1	218.3
HCF-EB-HBS	$\lg N + 24.8\lg\sigma_{max} = 70.5$	−0.863	387.9	524.4	127.6
HCF-HR-LBS	$\lg N + 22.2\lg\sigma_{max} = 63.1$	−0.837	361.8	504.3	41.3

Figure 10 shows the comparison of the fatigue *S-N* curves of the hot-rolled bonding specimens with that of the corresponding original plates, in which the symbol "O" means the specimens are processed from the original plates without surface polish. Previous studies [13,16] have reported the fatigue behavior of the original plates, which is also higher than the fatigue design curve of structural steel plate. As shown in Figure 10, the *S-N* curves of TC bimetallic steels with polished surfaces are naturally higher than those of corresponding original plates without polished surfaces, indicating that the improvement of surface roughness can significantly improve the fatigue properties. Moreover, the fatigue behavior of low bonding strength specimens with polished surfaces is higher than that of the high bonding strength specimens without polished surfaces when the fatigue life is larger than 3×10^5, indicating that the influence of bonding strength on fatigue behavior is less severe than that of surface roughness. It should be noted that the surface roughness has not been completely studied in these studies [13,16], so only the qualitative analysis is given herein.

Table 5 shows the expressions and some parameters regarding fatigue properties, in which the *r* is the Pearson correlation coefficient and the $\sigma_{2\times10^6}$ is the fatigue strength in terms of 2 million fatigue loading cycles. The fatigue, shear, and ultimate tensile strength of the hot-rolled TC bimetallic steel with high bonding strength are the highest among the three kinds of materials. The fatigue strengths corresponding to two million fatigue loading cycles for HCF-HR-HBS and HCF-HR-LBS are 401.9 MPa and 361.8 MPa, respectively, which means the high interface shear strength improves the fatigue strength by around 10%. While the fatigue strengths for HCF-EB-HBS are 387.9 MPa, which means the manufacturing methods have a limited effect on the fatigue strength. Considering the influence of the basic mechanical properties, the fatigue strengths were divided by the ultimate tensile strength, which is called the fatigue ratio *f*, as shown in Table 6. Generally, the fatigue ratio is the ratio of the fatigue limit or fatigue strength to the static tensile strength of a material, which can eliminate the impact of basic mechanical properties and indicate the normalized fatigue resistance of a material. It was indicated that the explosion-bonded TC bimetallic steel has a higher fatigue ratio than the hot-rolled steel, and the hot-rolled TC bimetallic steels tend

to have the same fatigue ratio despite the different bonding strengths. It can be concluded that the manufacturing methods, namely the explosive bonding process and hot-rolling process, have a great effect on the fatigue ratio, while the influence of the bonding strength is limited, which only improves the fatigue strength but not the fatigue ratio of the TC bimetallic steel. However, it should be noted that the fatigue ratio may not be the best parameter to measure the fatigue resistance of a material, and fatigue strength is still the most commonly used and intuitive parameter in engineering.

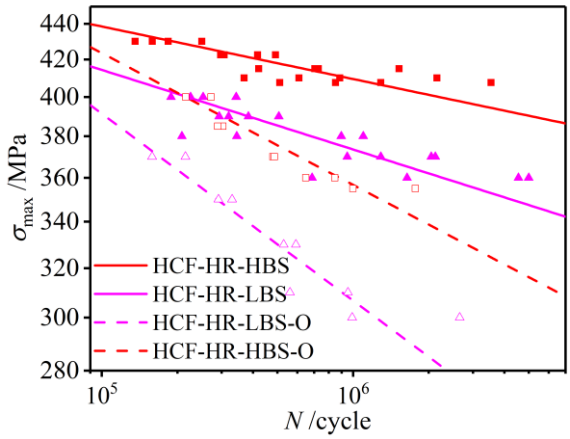


Figure 10. Comparison of the fatigue *S-N* curves between polished specimens and corresponding original plates.

Table 6. Comparison of the fatigue ratio.

Specimens	$\sigma_{2\times10^6}$ (MPa)	σ_u (MPa)	$f = \sigma_{2\times10^6}/\sigma_u$	Shear Strength (MPa)
HCF-HR-HBS	401.9	566.1	0.71	218.3
HCF-EB-HBS	387.9	524.4	0.74	127.6
HCF-HR-LBS	361.8	504.3	0.72	41.3

4. Conclusions

This paper presents a comparison of basic mechanical properties and high-cycle fatigue properties of three kinds of TC bimetallic steels with various interfacial conditions. Some conclusions and suggestions can be drawn:

1. Based on the comparison of stress-strain curves, it was found that different manufacturing methods and bonding degrees of the two component metals resulted in different nonlinear yield responses in the TC bimetallic steel.
2. The strength of the bonding interface affects the failure mode of the tensile coupons, but has only a slight effect on other tensile properties. In case of high bonding strength, the hot-rolled bonding TC bimetallic steel generally has higher tensile strengths and lower 0.2% proof strengths than the explosion-bonded one.
3. There were three failure modes that were characterized for the TC bimetallic steel in the high-cycle fatigue tests. The bonding interface and the surface roughness significantly affect their fatigue phenomena, and higher bonding strength may result in more failure modes in fatigue tests. Further research still needs to quantitatively study the relationship between fatigue life and the three failure modes.
4. The manufacturing methods significantly affect the fatigue ratio, on which the influence of the bonding strength is limited. The hot-rolled bonding TC bimetallic steel with high bonding strength has a 10% improvement in fatigue performance than the one with low bonding strength, while the manufacturing methods have almost no effect on the fatigue strength.

Author Contributions: Conceptualization, J.J.; Validation, H.B; Formal analysis, C.H.; Investigation, J.J., C.H. and L.H.; Resources, L.H.; Data curation, J.J.; Writing – original draft, C.H., J.J.; Writing – review & editing, H.B; Supervision, H.B; Funding acquisition, H.B. All authors have read and agreed to the published version of the manuscript.

Funding: This work was financially supported by the National Natural Science Foundation of China (52078272, 52108155), which is gratefully acknowledged.

Institutional Review Board Statement: Not applicable.

Informed Consent Statement: Not applicable.

Data Availability Statement: No new data were created.

Conflicts of Interest: The authors declare no conflict of interest.

References

1. *GB/T 8547-2019*; Administration of Quality Supervision, Inspection and Quarantine of People's Republic of China, Standardization Administration of China, Titanium Clad Steel Plates. China Standards Press: Beijing, China, 2019. (In Chinese)
2. Su, H.; Luo, X.; Chai, F.; Shen, J.; Sun, X.; Lu, F. Manufacturing Technology and Application Trends of Titanium Clad Steel Plates. *J. Iron Steel Res. Int.* **2015**, *22*, 977–982. [CrossRef]
3. Ban, H.; Shi, Y.; Tao, X. Use of clad steel in engineering structures. In Proceedings of the Fifteenth East Asia-Pacific Conference on Structural Engineering & Construction (EASEC-15), Xi'an, China, 11–13 October 2017; pp. 1167–1173.
4. Mousavi, S.A.; Al-Hassani, S.T.; Atkins, A.G. Bond strength of explosively welded specimens. *Mater Des.* **2008**, *29*, 1334–1352. [CrossRef]
5. Smith, L.M. *Engineering with Clad Steel*, 2nd ed.; Nickel Development Institute: Toronto, ON, Canada, 1994.
6. Yang, X.; Shi, C.G.; Fang, Z.H.; Sabuj, M.N. Application countermeasures of the manufacturing processes of titanium-steel composite plates. *Mater. Res. Express* **2018**, *6*, 026519. [CrossRef]
7. Shi, C.; Shi, H.; Fang, Z.; Sun, Z.; Feng, K.; Shao, F. Manufacturing Process and Interface Properties of Vacuum Rolling Large-Area Titanium-Steel Cladding Plate. *Russ. J. Non-Ferr. Met.* **2019**, *60*, 152–161.
8. Manikandan, P.; Hokamoto, K.; Deribas, A.A.; Raghukandan, K.; Tomoshige, R. Explosive welding of titanium/stainless steel by controlling energetic conditions. *Mater. Trans.* **2006**, *47*, 2049–2055. [CrossRef]
9. Liu, X.; Bai, R.; Uy, B.; Ban, H. Material properties and stress-strain curves for titanium-clad bimetallic steels. *J. Constr. Steel Res.* **2019**, *162*, 105756. [CrossRef]
10. Ban, H.; Bai, R.; Liu, M.; Liu, W.; Bai, Y. Study on the Material Properties and Constitutive Model of Titanium-Clad Steel. *Eng. Mech.* **2019**, *36*, 57–66. (In Chinese)
11. Seishiro, Y.; Takao, K.; Suzuki, K. Bonding Condition of Rolled Titanium Clad Steels. *Tetsu Hagane-J. Iron Steel Inst. Jpn.* **1986**, *72*, 671–677. (In Japanese)
12. Huang, C.; Ban, H.; Hai, L.; Jiang, J.; Shi, Y. Research on high-cycle fatigue properties of hot rolled titanium-clad bimetallic steel with low bonding strength. *J. Build. Struct.* **2022**, *43*, 36–43. (In Chinese)
13. Huang, C.; Ban, H.; Hai, L.; Shi, Y. Fatigue behaviour of titanium-clad bimetallic steel plate with different interfacial conditions. In Proceedings of the Tenth International Conference on Advances in Steel Structures (ICASS'2020), Chengdu, China, 21–23 August 2022; pp. 642–649.
14. Kurek, A.; Wachowski, M.; Niesłony, A.; Płociński, T. Fatigue tests and metallographic of explosively cladded steel-titanium bimetal. *Arch. Metall. Mater.* **2014**, *59*, 1565–1570. [CrossRef]
15. Karolczuk, A.; Kowalski, M.; Bański, R.; Żok, F. Fatigue phenomena in explosively welded steel–titanium clad components subjected to push–pull loading. *Int. J. Fatigue* **2013**, *48*, 101–108. [CrossRef]
16. Huang, C.; Hai, L.; Jiang, J.; Ban, H. High-cycle fatigue properties of explosion bonded titanium-clad bimetallic steel. *Int. J. Fatigue* **2023**, *169*, 107499. [CrossRef]
17. Sun, Q.; Zhang, X.; Zhang, G.; Cui, X.; Fan, H.; Tian, J. Researches on high cycle fatigue properties of TA2, Q345 and their explosively bonded plates. *Press. Vessel Technol.* **2019**, *36*, 9–17. (In Chinese)
18. *GB/T 3621-2007*; Administration of Quality Supervision, Inspection and Quarantine of People's Republic of China, Standardization Administration of China, Titanium and Titanium Alloy Plate and Sheet. China Standards Press: Beijing, China, 2007. (In Chinese)
19. *GB 50017-2017*; Ministry of Housing and Urban-Rural Construction of the People's Republic of China, Administration of Quality Supervision, Inspection and Quarantine of People's Republic of China, Standard for Design of Steel Structures. China Architecture & Building Press: Beijing, China, 2017. (In Chinese)
20. Smith, L.M. Engineering with clad steel. *Nickel Dev. Inst.* **2012**, *10064*, 1–24.
21. *GB/T 228.1-2010*; Administration of Quality Supervision, Inspection and Quarantine of People's Republic of China, Standardization Administration of China, Metallic Materials—Tensile Testing—Part 1: Method of Test at Room Temperature. China Standards Press: Beijing, China, 2010. (In Chinese)

22. *ISO 6892-1:2019*; The International Organization for Standardization(ISO), Metallic materials—Tensile testing—Part 1: Method of test at room temperature. The International Organization for Standardization (ISO): London, UK, 2019.
23. *GB/T 6396-2008*; Administration of Quality Supervision, Inspection and Quarantine of People's Republic of China, Standardization Administration of China, Clad steel plates-Mechanical and Technological Test. China Standards Press: Beijing, China, 2008. (In Chinese)
24. *GB/T 3075-2008*; Administration of Quality Supervision, Inspection and Quarantine of People's Republic of China, Standardization Administration of China, Metallic materials—Fatigue testing—Axial-Force-Controlled Method. China Standards Press: Beijing, China, 2008. (In Chinese)
25. Fronczek, D.M.; Saksl, K.; Chulist, R.; Michalik, S.; Wojewoda-Budka, J.; Sniezek, L.; Wachowski, M.; Torzewski, J.; Sulikova, M.; Sulova, K.; et al. Residual stresses distribution, correlated with bending tests, within explosively welded Ti gr. 2/A1050 bimetals. *Mater. Charact.* **2018**, *144*, 461–468. [CrossRef]
26. *EN 1993-1-9*; European Committee for Standardization (CEN), Eurocode 3, Design of Steel Structures—Part 1–9: Fatigue. Comité Européen de Normalisation: Brussels, Belgium, 2005.
27. *ANSI/AISC 360-16*; American Institute of Steel Construction, Specification for Structural Steel Buildings. American Institute of Steel Construction: Chicago, IL, USA, 2016.
28. *BS 7608:2014+A1:2015*; British Standards Institution, Guide to fatigue design and Assessment of Steel Products. British Standards Institution: London, UK, 2015.

Disclaimer/Publisher's Note: The statements, opinions and data contained in all publications are solely those of the individual author(s) and contributor(s) and not of MDPI and/or the editor(s). MDPI and/or the editor(s) disclaim responsibility for any injury to people or property resulting from any ideas, methods, instructions or products referred to in the content.